

tested for their affinities to CB₁ and CB₂ receptors, showing K_i values in the nanomolar range (Table 1). It is especially relevant that probes **1** and **2**, derived from ligand HU210, keep a high affinity for both cannabinoid receptors and that probe **3** keeps the selectivity feature of its parent compound, HU308, with high affinity for the CB₂ receptor whilst being inactive at the CB₁ receptor.

Table 1: Binding affinities of synthesized probes **1–3** to the CB₁ and CB₂ receptors.

Compound	K_i (CB ₁ R) [nM] ^[a]	K_i (CB ₂ R) [nM] ^[a]
1	2.4 ± 0.4	1.6 ± 0.4
2	11 ± 2	3 ± 1
3	> 5000	44 ± 4

[a] K_i values are given as the mean ± standard error from 2–3 independent experiments performed in triplicate.

To propose structural hypotheses for the binding of these compounds, we constructed three-dimensional models of the CB₁ and CB₂ receptors using the crystal structure of the homologous sphingosine 1-phosphate receptor 1 (S1P₁)^[11] as a template (the Supporting Information and Figure S1). Docking of ligands HU210 and HU308 into the receptor models (the Supporting Information and Figure S2) places the hydroxy groups pointing toward the extracellular environment. However, the entrance of the ligand into the binding pocket has been proposed very recently to be from the lipid bilayer, in particular through an opening between trans-membrane helices (TMs) 1 and 7 (Figure 1A).^[11] Thus, in ligand HU210, the hydroxy group attached to the phenyl ring is more distant to this opening than its allylic hydroxy group. As a consequence, probes **1** (Figure 1A,B) and **3** (Figure 1C) expand their biotin chains through this channel more favorably than probe **2** (not shown). Importantly, attachment of the biotin chain to ligands HU210 or HU308 decreases the binding affinity in a more pronounced manner in CB₁R than CB₂R (Table 1). According to the Ballesteros–Weinstein numbering scheme the side chains at positions 1.32 (Q in CB₁R and K in CB₂R), 1.35 (I in CB₁R and V in CB₂R), 7.34 (V in CB₁R and A in CB₂R), and 7.36 (A in CB₁R and A in CB₂R) define this channel between TMs 1 and 7. Thus, we hypothesize that this effect is due to the presence of amino acid residue K1.32 in the CB₂ receptor, which stabilizes the carbonyl group of the biotin chain in a more significant manner than residue Q1.32 of the CB₁ receptor.

Compounds **1–3** were used for *in vitro* labeling of cannabinoid receptors in transiently transfected hippocampal neuronal (HT22) cells (data not shown). In these experiments, probe **1** performed better than **2**, either because of the higher exposure of the biotin moiety as suggested by the computational model or because of the slightly higher affinity for CB₁R (Table 1). Therefore, we selected probes **1** and **3** for their use in native systems, and neurons and microglia were chosen as relevant systems for CB₁ and CB₂ receptors, respectively. Probe **1** is able to label neurons in primary culture (Figure 2A,B). Next, we checked the specificity of the labeling by parallel experiments in the presence of an excess

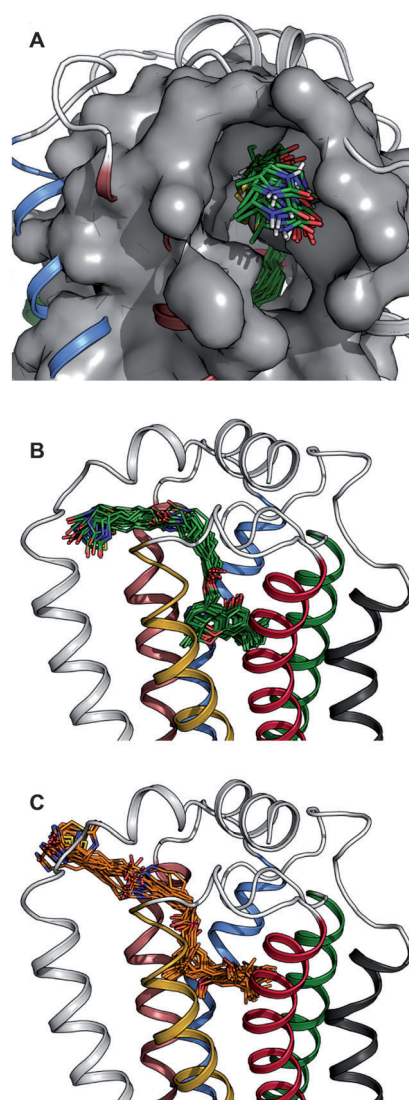


Figure 1. Molecular dynamics (MD) simulations of the ligand–receptor complexes (the Supporting Information). Molecular surface of the S1P₁-based homology model of the human CB₁R, showing the entrance/exit of the ligand to/from the binding pocket. The structures of probe **1** (in green, panels A and B) bound to CB₁R and probe **3** (in orange, panel C) bound to CB₂R are shown, computed during the MD trajectories. Helices color code: TM1 white, TM2 yellow, TM3 red, TM4 gray, TM5 green, TM6 blue, and TM7 brown.

of ligand HU210, which abolished labeling (Figure 2C). As expected, probe **3**, with no affinity for CB₁R, did not show any significant fluorescence in neurons (Figure 2D). Notably, this labeling is fully compatible with the simultaneous use of primary antibodies in colabeling studies (Figure 3). Probe **1** shows the predominant location of CB₁ receptor in the neuronal soma (Figure 3A), whereas the anti-MAP2 antibody labels the entire neuron (Figure 3B), including axon and dendrites, as expected from this marker. Labeling of CB₁ receptor by probe **1** (Figure 3D) is further confirmed by double staining with a commercial antibody against this receptor (Figure 3E,F).

To further explore the potential of the probes in a different native cell system, we assessed their performance in micro-

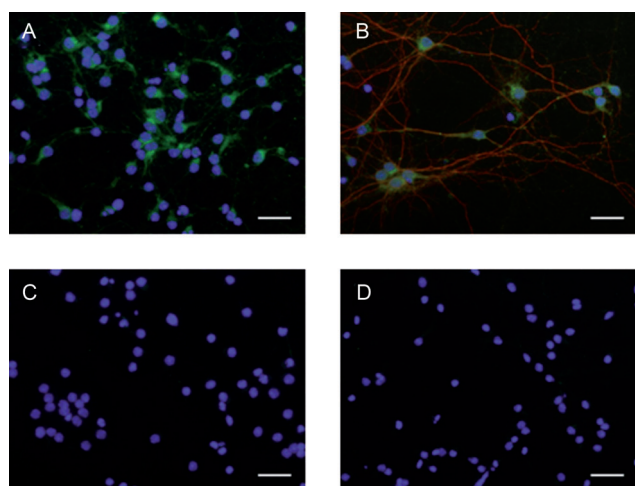


Figure 2. Labeling of CB₁R in neurons in primary culture with probe **1**. A) Neurons were incubated with **1** (0.5 μM). Excess of the probe was then removed, and the bound probe was detected with streptavidin-Alexa Fluor 488 (green). B) Colabeling of probe **1** and anti-MAP2 antibody (MAP2 = microtubule-associated protein 2) visualized with a secondary antibody conjugated to Alexa Fluor 594 (red). C) To assess specificity, cells were labeled with **1** (0.5 μM) in the presence of an excess of ligand HU210 (100 μM). D) Neurons incubated with the CB₂R-selective probe **3**. All samples were imaged under the same conditions by using a Zeiss fluorescence inverted microscope. Nuclei are shown in blue. Bars: 25 μm.

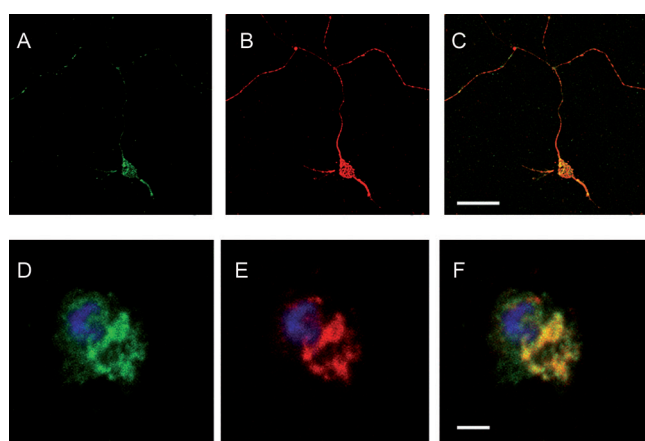


Figure 3. A–C) Double labeling of neurons with probe **1** (green, A) and with an anti-MAP2 antibody (red, B). Panel C shows merged image. D–F) Double labeling of neurons with probe **1** (green, D) and with an anti-CB₁R antibody (red, E). Panel F shows merged image. Images were obtained by using a Leica fluorescence confocal microscope. In D–F nuclei are shown in blue. Bars: 100 μm (A–C) and 5 μm (D–F).

glial cells, also known as the macrophages of the brain. These cells express CB₂R, which is believed to play a fundamental role in their immune-related functions.^[12] In agreement with the binding profile of the probes, both probes **1** and **3** allowed visualization of CB₂R in microglia (Figure 4A,B) but not in the presence of an excess of ligand HU210 (Figure 4C). Again, the intensity of the fluorescence signal is comparable with the one obtained with an antibody against the microglial marker Iba-1 (Figure 4D).

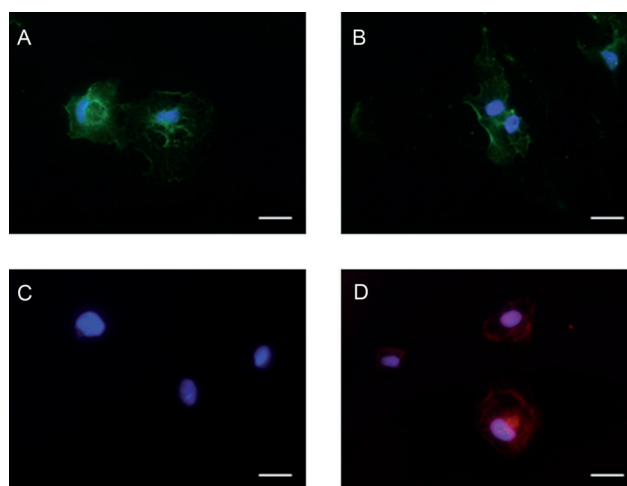


Figure 4. Labeling of CB₂R in rat microglial cells in primary culture with 0.5 μM of probes **1** (A) and **3** (B). Excess of the probe was then removed, and the bound probe was detected with streptavidin-Alexa Fluor 488 (green). C) To assess specificity, cells were labeled under the same conditions with the probe but in the presence of an excess of ligand HU210 (100 μM). D) Immunostaining of microglial cells with anti-Iba1 antibody (red, Iba1 = ionized calcium-binding adaptor molecule 1). All samples were imaged under the same conditions by using a Zeiss fluorescence inverted microscope. Nuclei are shown in blue. Bars: 25 μm.

Importantly, in microglial cells, labeling with probe **3** clearly reflects the changes in CB₂R expression between a resting state (Figure 5, panels A–C) and an activated (pro-inflammatory) phenotype induced by lipopolysaccharide (LPS) exposure (Figure 5, panels D–F).

Considering the relevance of the ECS in the regulation of the immune system we studied the potential of these probes in flow cytometry. The application of this methodology would facilitate the profiling of cannabinoid receptors at the single-

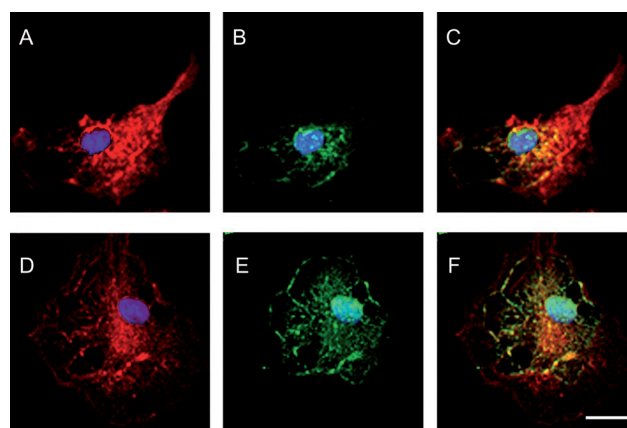


Figure 5. Labeling of CB₂R with probe **3** in rat microglial cells in resting (A–C) and activated (D–F) state after pro-inflammatory stimulus (LPS exposure). Microglia in primary culture were labeled with anti-Iba1 (in red, A and D) and with probe **3** (in green, B and E). Merged images are shown in panels C and F. Samples were imaged under the same conditions by using a Leica fluorescence confocal microscope. Nuclei are shown in blue. Bar (A–F): 5 μm.

cell level and could contribute to shed light on the function of the ECS in the immune system, a field of utmost current interest.^[13] Probes were tested in the monocytic cell line THP-1, which has been described to have a functional endocannabinoid system.^[14] Cells were incubated with probe **1** (1 μM) and then stained with streptavidin-Alexa Fluor 488 and analyzed by flow cytometry (Figure 6). Although the expression of CB₁ and CB₂ receptors is moderate in unstimulated THP-1 cells as assessed by western blot (data not shown), our experiments clearly demonstrate the suitability of probe **1** to visualize cannabinoid receptors in this cell line by flow cytometry.

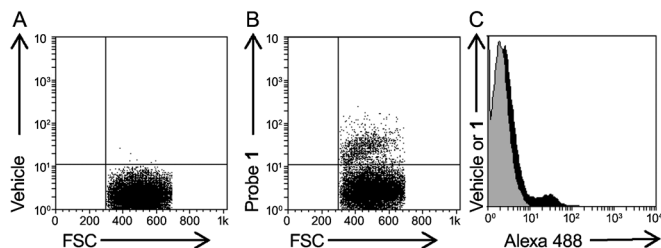


Figure 6. Flow cytometry analysis of THP-1 cells using probe **1**. Representative dot plots of THP-1 cells labeled with A) vehicle or B) probe **1**, followed by addition of streptavidin-Alexa Fluor 488. Forward scatter (FSC) indicates the size of the gated cells. C) Histograms display THP-1 cells stained with vehicle (gray) or probe **1** (black).

In conclusion, the probes described herein are, to our knowledge, the first small-molecule tools suitable for visualization of CB₁ and CB₂ receptors in native cell systems of physiological relevance with at least comparable potency to antibodies. Taking into account the practical limitations that these antibodies have, these probes increase the arsenal of chemical tools for the study of cannabinoid receptors and may help to dissect the complex roles of the ECS. Further extension of the versatility of this approach is currently ongoing.

Received: January 17, 2012
Revised: May 14, 2012
Published online: June 11, 2012

Keywords: bioorganic chemistry · cannabinoid ligands · chemical probes · membrane proteins · protein models

- [1] T. Bisogno, V. di Marzo, *CNS Neurol. Disord. Drug Targets* **2010**, 9, 564–573.
- [2] a) P. V. Chang, X. Chen, C. Smyrniotis, A. Xenakis, T. Hu, C. R. Bertozzi, P. Wu, *Angew. Chem.* **2009**, 121, 4090–4093; *Angew. Chem. Int. Ed.* **2009**, 48, 4030–4033; b) S. E. Tully, B. F. Cravatt, *J. Am. Chem. Soc.* **2010**, 132, 3264–3265; c) J. W. Chang, R. E. Moellering, B. F. Cravatt, *Angew. Chem.* **2012**, 124, 990–994; *Angew. Chem. Int. Ed.* **2012**, 51, 966–970.
- [3] N. L. Grimsey, C. E. Goodfellow, E. L. Scotter, M. J. Dowie, M. Glass, E. S. Graham, *J. Neurosci. Methods* **2008**, 171, 78–86.
- [4] a) A. S. Yates, S. W. Doughty, D. A. Kendall, B. Kellam, *Bioorg. Med. Chem. Lett.* **2005**, 15, 3758–3762; b) M. Bai, M. Sexton, N. Stella, D. J. Bornhop, *Bioconjugate Chem.* **2008**, 19, 988–992; c) M. Sexton, G. Woodruff, E. A. Horne, Y. H. Lin, G. G. Muccioli, M. Bai, E. Stern, D. J. Bornhop, N. Stella, *Chem. Biol.* **2011**, 18, 563–568; d) R. R. Petrov, M. E. Ferrini, Z. Jaffar, C. M. Thompson, K. Roberts, P. Diaz, *Bioorg. Med. Chem. Lett.* **2011**, 21, 5859–5862.
- [5] L. Martín-Couce, M. Martín-Fontecha, S. Capolicchio, M. L. López-Rodríguez, S. Ortega-Gutiérrez, *J. Med. Chem.* **2011**, 54, 5265–5269.
- [6] a) W. A. Devane, A. Breuer, T. Sheskin, T. U. Järbe, M. S. Eisen, R. Mechoulam, *J. Med. Chem.* **1992**, 35, 2065–2069; b) A. C. Howlett, F. Barth, T. I. Bonner, G. Cabral, P. Casellas, W. A. Devane, C. C. Felder, M. Herkenham, K. Mackie, B. R. Martin, R. Mechoulam, R. G. Pertwee, *Pharmacol. Rev.* **2002**, 54, 161–202.
- [7] L. Hanus, A. Breuer, S. Tchilibon, S. Shiloah, D. Goldenberg, M. Horowitz, R. G. Pertwee, R. A. Ross, R. Mechoulam, E. Fride, *Proc. Natl. Acad. Sci. USA* **1999**, 96, 14228–14233.
- [8] R. Mechoulam, N. Lander, A. Breuer, J. Zahalka, *Tetrahedron: Asymmetry* **1990**, 1, 315–318.
- [9] G. Appendino, A. Minassi, N. Daddario, F. Bianchi, G. C. Tron, *Org. Lett.* **2002**, 4, 3839–3841.
- [10] K. Ishihara, M. Nakayama, S. Ohara, H. Yamamoto, *Tetrahedron* **2002**, 58, 8179–8188.
- [11] M. A. Hanson, C. B. Roth, E. Jo, M. T. Griffith, F. L. Scott, G. Reinhart, H. Desale, B. Clemons, S. M. Cahalan, S. C. Schuerer, M. G. Sanna, G. W. Han, P. Kuhn, H. Rosen, R. C. Stevens, *Science* **2012**, 335, 851–855.
- [12] N. Stella, *Neuropharmacology* **2009**, 56, 244–253.
- [13] R. Tanasescu, C. S. Constantinescu, *Immunobiology* **2010**, 215, 588–597.
- [14] S. Q. Xie, A. Borazjani, M. J. Hatfield, C. C. Edwards, P. M. Potter, M. K. Ross, *Chem. Res. Toxicol.* **2010**, 23, 1890–1904.